Differential Scanning Calorimetric Studies of Photosystem II: Evidence for a Structural Role for Cytochrome b_{559} in the Oxygen-Evolving Complex†

Lynmarie K. Thompson, Julian M. Sturtevant, and Gary W. Brudvig*,‡
Department of Chemistry, Yale University, New Haven, Connecticut 06511
Received April 14, 1986; Revised Manuscript Received June 24, 1986

ABSTRACT: Differential scanning calorimetry (DSC) has been used to investigate the macroscopic structure of photosystem II (PS II). Five endothermic transitions, A_1, A_2, B, C, and D, are observed in the 30–70 °C temperature range and are partially assigned on the basis of heat inactivation experiments, relative peak areas, and the effect of $MgCl_2$ on the DSC trace. We suggest that peaks C and D correspond to the denaturation of the light-harvesting chlorophyll *a*/*b* proteins and peak B to the denaturation of components critical to the electron-transport chain. In a DSC study of thylakoid membranes [Cramer, W. A., Whitmarsh, J., & Low, P. S. (1981) *Biochemistry 20*, 157–162], the lowest temperature shoulder was assigned to the denaturation of the oxygen-evolving complex (OEC). By correlating the temperature of heat inactivation with the temperatures of the DSC peaks of PS II in a range of detergent concentrations (causing shifts in the peak positions), we assign peak A_2 to the functional denaturation of the OEC. We have used peak A_2 as a new probe of the OEC and have found this peak to be sensitive to the oxidation state of cytochrome b_{559}. Oxidation of cytochrome b_{559} with 1 mM ferricyanide, which has no effect on oxygen evolution activity, causes peak A_2 to disappear, probably by making it too broad to observe. In contrast, inhibitory treatments such as the removal of the 17-, 23-, and 33-kilodalton polypeptides and/or Mn by treatments with 2 M NaCl or 0.8 M tris(hydroxymethyl)aminomethane, all of which also lead to the oxidation of cytochrome b_{559}, cause no further changes in the DSC trace. Oxidation of cytochrome b_{559} apparently decreases the cooperativity of the denaturation of component(s) critical to oxygen evolution activity, which indicates that cytochrome b_{559} plays a significant role in the macroscopic structure of the OEC.

Differential scanning calorimetry (DSC)[1] monitors the heat capacity of a system as a function of temperature. DSC has been used to study complex, multicomponent membrane systems, such as erythrocyte membranes (Brandts et al., 1977, 1978; Lysko et al., 1981), to obtain information about specific components in the system, by monitoring the effects of changes in conditions on particular DSC peaks. In complex systems such as this one, a peak in the DSC trace will usually correspond to the cooperative unfolding of a protein domain. This macroscopic tool is similarly well suited to the study of photosystem II (PS II), a multiprotein membrane complex in which the roles of the individual proteins are not well understood. DSC can be used both to investigate the macroscopic structure of PS II as a whole and to investigate the structure and function of the parts of the complex by monitoring changes in particular DSC peaks which are assigned to particular components. Cramer et al. (1981) examined the DSC behavior of thylakoid membranes and suggested that a low-temperature shoulder in the DSC trace corresponds to the denaturation of the oxygen-evolving complex (OEC). We have focused on this peak, which can be much better resolved in our DSC study of PS II, in order to use DSC as a new probe of the OEC.

Neither the overall structure of the PS II complex nor the roles of the component proteins in the structure and in the catalysis of electron transport and oxygen evolution are well understood. Photosystem II is composed of a reaction-center core complex coupled to an antenna of chlorophyll (Chl) molecules, which are bound by the light-harvesting Chl *a*/*b* proteins (LHCP). The function of the Chl antenna is to trap light energy and funnel it to the reaction center. PS II membranes (Berthold et al., 1981) contain 200–250 Chl per reaction center. About 50 Chl are associated with the core complex (Satoh, 1983), and the remaining 150–200 are the antenna Chl. The number of Chl bound by each LHCP is uncertain; values ranging from 6 to 13 Chl/LHCP have been reported (Zuber, 1985). In order to make a rough estimate of the molecular weight and composition of PS II, we have assumed 10 Chl/LHCP, which suggests a stoichiometry of 15–20 LHCP per core complex. The core complex is composed of numerous membrane proteins, which are usually referred to by their approximate (from SDS–PAGE) molecular weights of 47K, 43K, 34K, 32K, 22K, 9K, and 4K (two copies each of the latter two) and several extrinsic proteins, of 33K, 23K, 17K, and 10K (Tang & Satoh, 1985; Ikeuchi et al., 1985; Ljungberg et al., 1984; Babcock et al., 1985). There are at least two species of LHCP, with molecular weights of about 25K and 27K (Larsson & Andersson, 1985). An estimate of the total molecular weight of the core complex, calculated from the exact molecular weights derived from gene sequences when available (Critchley, 1985; Herrmann et al., 1984), and including the 50 core Chl (45 kDa), is about 365K. The total molecular weight of the LHCP and its bound Chl associated with each core complex is 525–700 K. This rough

† Supported by National Institutes of Health Grant GM32715.
‡ Searle Scholar (1983–1986), Camille and Henry Dreyfus Teacher/Scholar (1985–1990), and Alfred P. Sloan Foundation Research Fellow (1986–1988).

[1] Abbreviations: Chl, chlorophyll; DCIP, 2,6-dichlorophenolindophenol; DCMU, 3-(3,4-dichlorophenyl)-1,1-dimethylurea; DPC, *sym*-diphenylcarbazide; DSC, differential scanning calorimetry; EDTA, ethylenediaminetetraacetic acid; EPR, electron paramagnetic resonance; HEPES, *N*-(2-hydroxyethyl)piperazine-*N*′-2-ethanesulfonic acid; kDa, kilodalton(s); LHCP, light-harvesting Chl *a*/*b* proteins; MES, 2-(*N*-morpholino)ethanesulfonic acid; OEC, oxygen-evolving complex; PS II, photosystem II; P680, primary electron donor in PS II; SDS–PAGE, sodium dodecyl sulfate–polyacrylamide gel electrophoresis; Tris, tris(hydroxymethyl)aminomethane; TX-100, Triton X-100.

0006-2960/86/0425-6161$01.50/0

calculation shows that PS II membranes are about 59–66% LHCP by mass, which suggests that the DSC trace of PS II membranes may be dominated by the denaturation profile of the LHCP.

Since our chief interest is in the proteins of the core complex, specifically those involved in oxygen evolution, we have focused this DSC study on the low-temperature peak first observed by Cramer et al. (1981). We have verified that this peak involves the denaturation of components essential to oxygen evolution. Unfortunately, the identity of the proteins which constitute the OEC—those which may be undergoing denaturation at this peak—is unknown. Although there is evidence that a manganese complex is the site which stores the oxidizing equivalents used in catalysis [reviewed by Amesz (1983)], the identities of the Mn binding proteins have not been determined. The 33-, 23-, and 17-kDa extrinsic polypeptides appear to mediate the requirements for the cofactors calcium and chloride, and the 33-kDa polypeptide stabilizes the Mn complex (Miyao & Murata, 1984, 1985; Ghanotakis et al., 1984b). Cytochrome b_{559} is one of the cofactors present in PS II whose function is unknown. Various roles have been proposed for it [reviewed by Cramer & Whitmarsh (1977)], including a role in oxygen evolution. There are two copies of cytochrome b_{559} per PS II core (Lam et al., 1983; de Paula et al., 1985). It is bound by the 9-kDa polypeptide and is postulated to be coordinated by two histidine ligands. Since the 9-kDa polypeptide contains only one histidine, the other is thought to be provided either by a second copy of the 9-kDa protein or by a 4-kDa protein (Babcock et al., 1985; Herrmann et al., 1984). These components, thought to be important to the OEC, can be perturbed by several inhibitory treatments. Treatments such as removing the extrinsic polypeptides and Mn, and altering the redox potential and oxidation state of cytochrome b_{559}, can be used to investigate the proteins involved in the low-temperature DSC peak.

The effect of heat on thylakoid membranes and on PS II has been extensively studied by methods other than DSC. These studies have examined heat-induced changes in both membrane structure and function. It has been found that heat treatments cause destacking of thylakoid membranes (Gounaris et al., 1983) and dissociation of some of the LHCP from the PS II core complex (Armond et al., 1980; Sundby & Andersson, 1985). Functional studies have shown that oxygen evolution is more sensitive to heat inactivation than is the remainder of the electron-transport chain (Katoh & San Pietro, 1967). The denaturation of the OEC seems to correlate with the release of two Mn and with the conversion of cytochrome b_{559} from its native high-potential form (E_m = 370 mV) to low-potential forms (E_m = 60–80 mV) (Cramer et al., 1981; Nash et al., 1985). A recent study indicates that the loss of activity upon heat treatment precedes the release of the extrinsic polypeptides (Nash et al., 1985). We have utilized heat inactivation experiments to augment this DSC study, by using DSC to answer questions which have been raised by heat inactivation experiments and by using heat inactivation to aid in assigning DSC peaks.

The goal of this investigation of the denaturation of the OEC is to develop DSC as a new probe of the OEC and to use it to determine what components—cofactors and proteins—are involved in the catalysis of oxygen evolution. We have assigned several of the endothermic transitions by examining the effects of various treatments on the DSC peaks and by correlating the peaks with heat inactivation. We have focused on the low-temperature endotherm, peak A_2, which we have shown to correspond to the OEC and to be highly sensitive to changes in cytochrome b_{559}. These studies provide evidence that cytochrome b_{559} plays a structural role in the oxygen-evolving complex.

Experimental Procedures

PS II membranes were prepared from spinach leaves by the methods described previously [Berthold et al. (1981) as modified by Beck et al. (1985)] and then washed repeatedly by centrifugation in the final buffer of the above procedure, which will be called pH 6 buffer [20 mM MES–NaOH, pH 6.0, 15 mM NaCl, 5 mM $MgCl_2$, and 30% (v/v) ethylene glycol (included as a cryoprotectant)], to remove residual TX-100. In all cases, washing refers to resuspension of the PS II pellet in the specified buffer and centrifugation at 35000*g* for 10 min, discarding the supernatant. The PS II membranes were then washed twice in pH 6 buffer plus 0.01% TX-100 (to ensure a constant TX-100 concentration in DSC samples) and stored at 77 K. All manipulations of PS II samples prior to the loading of the calorimeter (except as noted) were performed at 4 °C in dim green light. Oxygen evolution assays were performed with a Clark-type oxygen electrode in a buffer consisting of 25 mM MES–NaOH, pH 6.5, and 10 mM NaCl, with 250 μM 2,5-dichloro-*p*-benzoquinone and 3.5 mM $K_3Fe(CN)_6$ as electron acceptors. The activities of the preparations used in these experiments were 300–600 μmol of O_2 evolved h^{-1} (mg of Chl)$^{-1}$. Neither the activities nor the polypeptide compositions were significantly altered by the washing to remove TX-100.

Salt washing, to remove the 17- and 23-kDa polypeptides (Ghanotakis et al., 1984a), was performed by resuspending a PS II pellet to about 0.5 mg of Chl/mL in 2 M NaCl, 20 mM MES–NaOH, pH 6.0, and 30% ethylene glycol. This solution was stirred 45 min, pelleted by centrifugation, washed once in the salt wash buffer, and then washed several times in pH 6 buffer. Tris washing, to remove the 17-, 23-, and 33-kDa polypeptides and Mn (Kuwabara & Murata, 1983), was preformed in 0.8 M Tris-HCl, pH 8.0, again at 0.5 mg of Chl/mL. The solution was stirred 20 min under room light, washed once with pH 6 buffer plus 1 mM EDTA to remove Mn, and then washed several more times in pH 6 buffer.

The polypeptide composition of PS II samples was determined by SDS–PAGE on a 12.5% acrylamide gel according to the procedures of Chua (1980) as modified by Ikeuchi et al. (1985). Removal of the appropriate polypeptides was verified by densitometer scans of the gels. Oxygen evolution activities of the treated PS II membranes were similar to published values (Ghanotakis et al., 1984a; Kuwabara & Murata, 1983): 2 M NaCl washed samples retained 29% activity, which rose to 83% upon addition of 5 mM $CaCl_2$. Tris-washed samples showed 3–7% of control oxygen evolution activity.

Oxidation and reduction of cytochrome b_{559} were performed by washing twice in pH 6 buffer plus 1 mM ferricyanide and 1 mM ascorbate, respectively. Samples with no $MgCl_2$ were prepared by two washes in 10 mM MES–NaOH, pH 6.0, and 5 mM EDTA followed by two washes in pH 6 buffer with 0.01% TX-100, but with no $MgCl_2$. Good resolution of peaks A_2 and B, which was needed for the correlation of DSC peaks with heat inactivation temperatures, was obtained in pH 7.5 buffer (20 mM HEPES–NaOH, pH 7.5, 15 mM NaCl, 5 mM $MgCl_2$, and 30% ethylene glycol). All samples were washed at least twice in the buffer to be used for the DSC measurement. The final supernatant was used both for the final resuspension and as a reference, in order to ensure an exact concentration match of all components other than PS II in the sample and reference cell of the calorimeter.

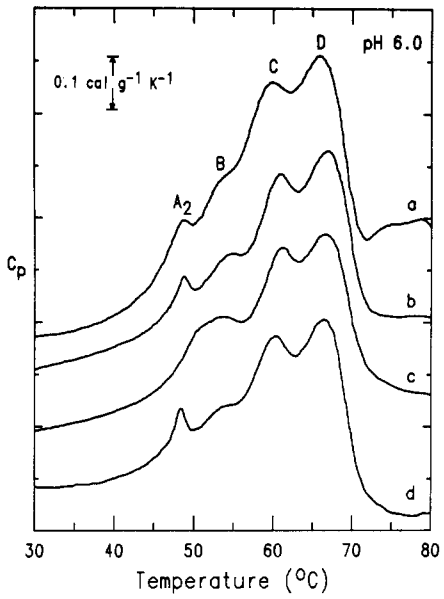

FIGURE 1: Tracings of DSC scans of three different PS II preparations in pH 6 buffer plus 0.01% TX-100. (a) Preparation 1; (b and c) preparation 2; (d) preparation 3; sample concentrations 1.4–2.1 mg of Chl/mL. Peaks A_2, B, C, and D are resolved under these conditions.

Calorimetric experiments were conducted in a Russian-built DASM-4 differential scanning calorimeter (Privalov, 1980) at a scan rate of 1 °C/min. The quality of the base lines obtained with PS II was quite variable. Some scans contained exotherms at low temperatures (20–35 °C), which we could not explain, reproduce, or consistently eliminate. Sample concentrations were 1–2 mg of Chl/mL. The heat capacity scales of the figures were computed by assuming 230 Chl/PS II, which yields 207-kDa Chl/995-kDa PS II (protein + Chl).

Heat inactivation studies were performed by incubating aliquots of a PS II sample (same concentration as was used for DSC) in a temperature bath which was heated at approximately 1 °C/min. Aliquots were withdrawn at appropriate temperatures, placed on ice, and later assayed for activity. Electron-transport activity from water or from the artificial electron donor DPC to the electron acceptor DCIP was measured spectrophotometrically. The assay buffer contained 25 mM MES–NaOH, pH 6.5, 10 mM NaCl, 0.001% TX-100, 30 μM DCIP, and, where indicated, 0.5 mM DPC.

Results

A comparison of the DSC traces of several different PS II preparations (Figure 1) shows the reproducibility which can be obtained if the residual TX-100 concentration is kept constant. A theoretical fit to the DSC curve obtained under these conditions was calculated by the method described by Edge et al. (1985). This method assumes that each denaturation is a two-state process at equilibrium, which requires that its equilibrium constant obey the van't Hoff equation:

$$\left(\frac{\partial \ln K}{\partial T}\right)_P = \frac{\Delta H_{vH}}{RT^2}$$

Obviously, this analysis assumes reversibility, which we have not been able to demonstrate (upon heating and reheating a sample through one transition at a time, the reheating scans contain no endothermic transitions). However, it has been argued that at least in some cases equilibrium thermodynamics can be applied to the interpretation of the DSC behavior of seemingly irreversible denaturations of proteins and that perhaps their apparent irreversibility is due to an extremely slow renaturation (Manly et al., 1985). In order to account

Table I: Thermodynamic Parameters Used for the Calculated DSC Curve in Figure 2

peak	$t_{1/2}$ (°C)	Δh_{cal} (cal/g)	% Δh_{cal}	β^a (g/mol)
A_1	47.24	0.96	16	45 500
A_2	48.18	0.10	2	2 995 000
B	53.66	0.95	16	74 100
C	59.94	1.74	30	52 500
D	66.30	2.11	36	46 900

[a] $\beta = \Delta H_{vH}/\Delta h_{cal}$ = molecular weight of the cooperative unit (Sturtevant, 1974).

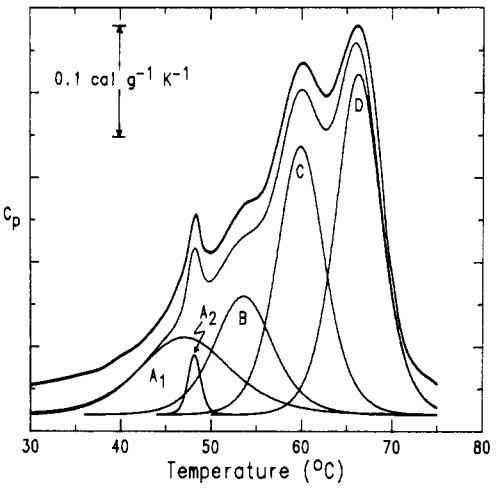

FIGURE 2: Computer fit to the DSC curve of PS II preparation 3 (top boldface curve is experimental trace). The five endothermic components are shown beneath the summed curve and arbitrarily named A_1, A_2, B, C, and D.

for the major peaks, we have assumed five independent denaturation steps. The three parameters for each transition, Δh_{cal}, ΔH_{vH}, and $t_{1/2}$, are initially estimated from the data after drawing five reasonable peaks: Δh_{cal}, the specific calorimetric enthalpy in calories per gram, is evaluated as the area under the peak; ΔH_{vH}, the van't Hoff enthalpy, is evaluated with the equation

$$\Delta H_{vH} = 4RT_m^2 \frac{c_{ex}^{max}}{\Delta h_{cal}}$$

where T_m is the absolute temperature of the maximum of the peak and c_{ex}^{max} is the maximum excess specific heat; $t_{1/2}$, the temperature in degrees centigrade of half-denaturation, is estimated as t_m. The parameters are varied systematically to minimize the standard deviation between the calculated and the observed DSC curves. The parameters which produce the best fit for curve d in Figure 1 are presented in Table I; the standard deviation is 1.7% of the maximal value of the excess specific heat. The calculated component curves for the five peaks (A_1, A_2, B, C, and D) and their sum are shown with the experimental DSC trace (top boldface curve) in Figure 2.

Only four of these calculated component peaks are resolved experimentally under these conditions (pH 6.0, 0.01% TX-100). The t_m values for these peaks, the averages of the values for four different preparations, are as follows: A_2 occurs at 49.1 ± 0.8 °C, B occurs at 54.0 ± 0.2 °C, C occurs at 60.8 ± 0.4 °C, and D occurs at 66.5 ± 0.1 °C. The temperature of peak A_2 is most variable, as was also found by Cramer et al. (1981) in their DSC study of thylakoid membranes. The t_m of peak A_2 can even change slightly between two seemingly identical samples from the same preparation (see the two traces, curves b and c, shown for preparation 2 in Figure 1). This variability of peak A_2 may be related to the fraction of

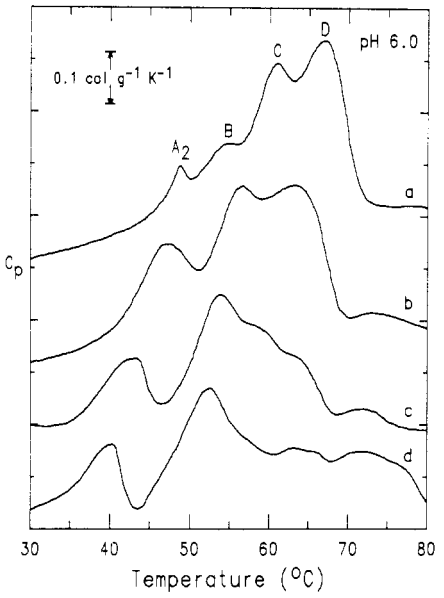

FIGURE 3: Effect of detergent on the DSC behavior at pH 6.0. DSC scans of PS II preparation 2 in pH 6 buffer plus (a) 0.01% TX-100, (b) 0.03% TX-100, (c) 0.05% TX-100, and (d) 0.1% TX-100; sample concentrations 1.4–2.1 mg of Chl/mL.

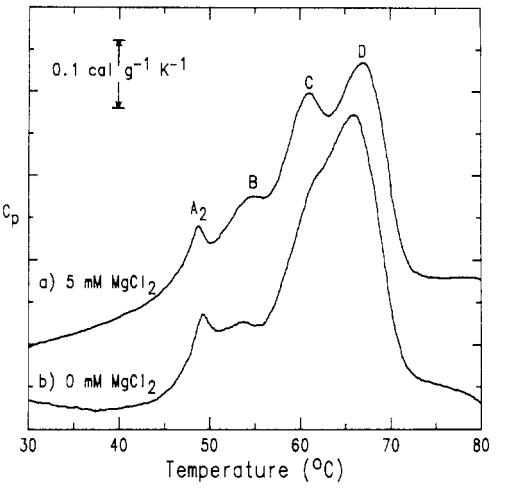

FIGURE 4: Cation-induced stacking effect on peak C. PS II preparation 2 in (a) pH 6 buffer, which contains 5 mM $MgCl_2$, plus 0.01% TX-100 (1.8 mg of Chl/mL) and (b) the same buffer with no $MgCl_2$ (1.3 mg of Chl/mL).

cytochrome b_{559} which is present in the low-potential forms, since this fraction is known to vary among different preparations (Lam et al., 1983; Sandusky et al., 1983) and to be increased by aging (Cramer & Whitmarsh, 1977). An EPR quantitation (de Paula et al., 1985) of the oxidized cytochrome b_{559} signals of one of our preparations showed 25% low-potential cytochrome b_{559}. Samples which were not extensively washed to remove TX-100 contained much less low-potential cytochrome b_{559}; perhaps the extensive washing to remove detergent may remove some of the 17- and 23-kDa polypeptides, which causes the conversion of the high- to the low-potential forms (Larsson et al., 1984). We have varied the fraction of low-potential cytochrome b_{559} by mixing control and salt-washed samples in several ratios and have observed changes in the position of peak A_2. In a sample containing 80% control and 20% salt-washed PS II, the position of peak A_2 was shifted by 2 °C relative to the control (results not shown). Thus, the observed variations in the temperature of peak A_2 in untreated samples can be accounted for by small variations in the fraction of low-potential cytochrome b_{559}. The variations in the temperature of peak A_2 in untreated samples are quite small relative to the changes in this peak caused by treatments which we report below.

The dramatic effects of detergent on the DSC trace (within the concentration range 0.01–0.1% TX-100, which causes no irreversible inhibition of oxygen evolution) are shown in Figure 3. The shifts of peaks to lower temperatures (decrease in t_m) in the presence of higher detergent concentrations suggest an increase in the stability of the denatured protein. At high detergent concentrations, peak B is no longer resolved. Due to the increased size of the low-temperature peak, we suggest it is composed of peaks A_1, A_2, and B. Further support for this assignment will be presented below. Other effects of increasing detergent concentrations on the DSC trace include the broadening of peak D and the exposure of small peaks in the 62–67 °C range which are buried under peak D at a lower percentage of TX-100. In the past, the residual TX-100 concentration has not usually been controlled during manipulations of PS II by various workers. Most treatments involve repeated centrifugation and resuspension in various buffers, which will result in washing out the TX-100. Therefore, the effects both of the treatment and of the decreased percentage of TX-100 will be observed. In particular, this may account for the inconsistent heat inactivation results which have been obtained by various workers, as cited recently by Nash et al. (1985).

On the basis of the large sizes of peaks C and D, we suggest that they correspond to the denaturation of the major component of the PS II complex, the LHCP. Although the LHCP are poorly characterized, it seems that there are at least two distinct polypeptides (Larsson & Andersson, 1985). The two DSC peaks may each be due to the denaturation of one of these proteins. If we assume that all proteins involved denature with approximately the same specific enthalpy [the typical enthalpy range observed for globular proteins with a t_m between 30 and 70 °C is 1–9 cal/g (Privalov, 1979)], then the relative sizes of the DSC peaks can be roughly correlated with the relative masses of the proteins whose denaturations they represent. As shown in Table I, peaks C and D account for approximately 66% of the total enthalpy of the PS II denaturation. On the basis of the polypeptide composition of PS II discussed above, LHCP constitute 59–66% of the total mass of the PS II complex. This suggests that peaks C and D represent the denaturation of the LHCP. The effect of magnesium on peak C provides additional evidence for the assignment of this endotherm to the denaturation of the LHCP. Figure 4 shows that 5 mM $MgCl_2$ causes a sharpening of peak C, indicating a more cooperative denaturation. The stacking of thylakoid membranes has been shown to be mediated by the LHCP and can be induced by cations, 2–5 mM Mg^{2+} or 100–150 mM Na^+ or K^+ (Mullet & Arntzen, 1980). In addition, fluorescence experiments have shown that some PS II complexes in thylakoid membranes are capable of excitation energy transfer to neighboring complexes and that these interactions are promoted by magnesium (Melis & Homann, 1978). Since magnesium promotes both stacking and energy transfer, it probably increases intermolecular interactions among the LHCP, which might increase the cooperativity of LHCP denaturation. This is consistent with the $MgCl_2$-induced sharpening of peak C observed in Figure 4.

By correlating the heat inactivation of oxygen evolution with DSC behavior under various conditions, we have demonstrated that the functional denaturation of the OEC occurs at peak A_2. This was first suggested by Cramer et al. (1981), who observed a shoulder at 42–44 °C in DSC scans of thylakoid membranes. They showed that at this temperature the fol-

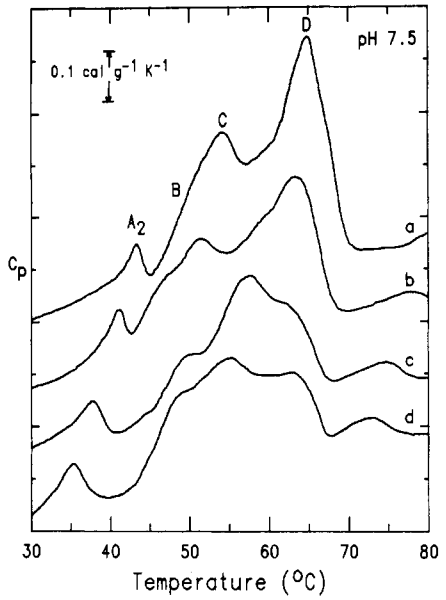

FIGURE 5: Effect of detergent on the DSC behavior at pH 7.5. DSC scans of PS II preparation 4 in pH 7.5 buffer plus (a) 0.01% TX-100, (b) 0.03% TX-100, (c) 0.05% TX-100, and (d) 0.1% TX-100; sample concentrations 1.3–1.4 mg of Chl/mL.

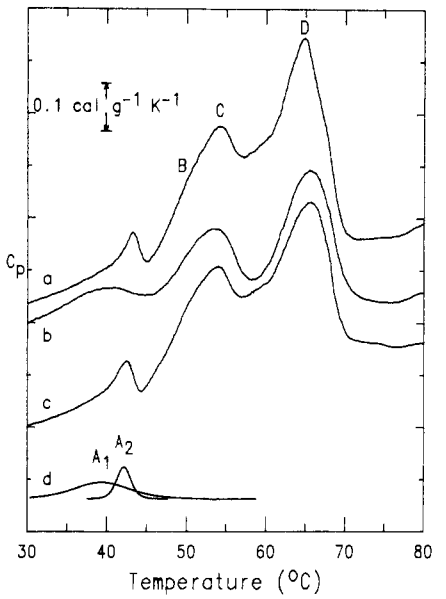

FIGURE 6: Effect of the oxidation state of cytochrome b_{559} on DSC behavior. Experimental DSC scans of PS II preparation 4 at 0.01% TX-100: (a) control; (b) oxidized (washed twice into pH 7.5 buffer plus 1 mM ferricyanide); (c) rereduced (sample b washed twice into pH 7.5 buffer plus 1 mM ascorbate and then into pH 7.5 buffer); sample concentrations 1.3–1.4 mg of Chl/mL. Calculated DSC curves: (d) the component peaks A_1 and A_2, calculated to fit trace c (after base-line correction).

lowing denaturation occurs: loss of oxygen evolution activity, conversion of high-potential to low-potential cytochrome b_{559}, and release of two Mn per PS II. Since this peak is much better resolved in our DSC traces of PS II, it is an ideal system for demonstrating the correlation between peak A_2 and loss of oxygen evolution. The possibility that the peak and the denaturation occur at the same temperature by mere coincidence can be reduced by manipulating the DSC conditions to shift peak A_2 and showing that the temperature of activity loss shifts similarly. We have done this by utilizing the t_m shifts induced by TX-100 at pH 7.5, as shown in Figure 5. Under these conditions, peak A_2 remains resolved from peak B throughout the range of detergent concentrations. However,

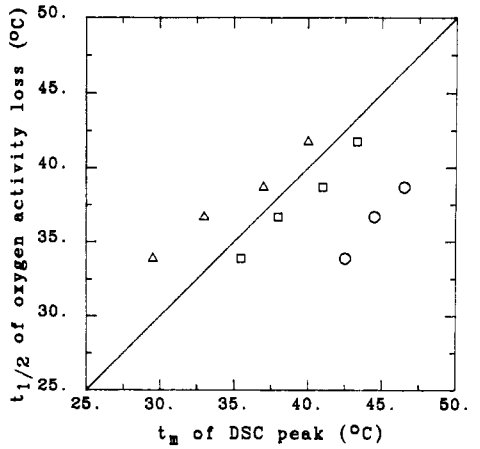

FIGURE 7: Correlation of the DSC peak temperatures (t_m from Figure 5) with heat inactivation temperatures ($t_{1/2}$, temperature of half-inactivation, determined for samples equivalent to those of Figure 5). For each sample, $t_{1/2}$ is plotted vs. the t_m of the DSC peak A_1 (△), A_2 (□), and B (○). Note that the coincidence of $t_{1/2}$ and t_m occurs along the diagonal shown.

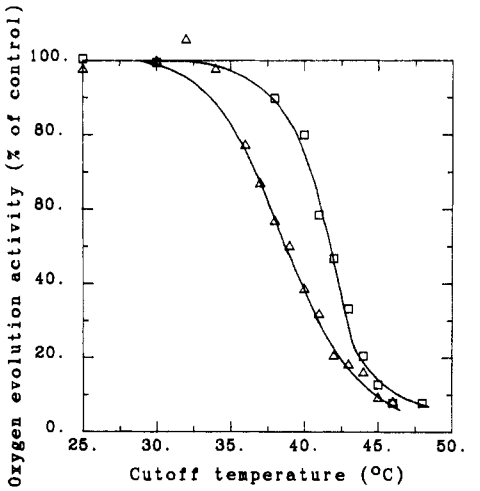

FIGURE 8: Effect of the oxidation state of cytochrome b_{559} on heat inactivation: remaining oxygen evolution activity (percent of control) vs. temperature at which the aliquot was withdrawn from the heating bath, plotted for samples equivalent to those of Figure 6, with reduced [control (□)] and oxidized (△) cytochrome b_{559}.

peaks A_1 and A_2 remain unresolved. Oxidation of cytochrome b_{559} removes peak A_2 (Figure 6, to be discussed below) and leaves a broad peak at slightly lower temperature. A computer fit to the DSC trace of the sample with cytochrome b_{559} reduced (Figure 6, trace c) can be used to resolve the component curves for peaks A_1 and A_2 (Figure 6, trace d). The similarity between the broad peak of the oxidized trace and the A_1 peak calculated for the reduced trace suggests that the broad peak is A_1, which is not changed significantly by oxidation of cytochrome b_{559}. Thus, we have assigned the t_m of peak A_1 for each detergent concentration by oxidation of cytochrome b_{559} (results not shown). We have performed a heat inactivation study of samples identical with the DSC samples of Figure 5 and have plotted in Figure 7 the $t_{1/2}$ of activity loss vs. the t_m for peaks A_1, A_2, and B. Destruction of the OEC clearly does not correlate with peak B but does correlate well with peaks A_1 and/or A_2. We argue that peak A_2 is more likely to represent the denaturation of the OEC because of the following: (1) the temperature range of the loss of activity (38–46 °C; see Figure 8, control sample) corresponds better to peak A_2 (40–45 °C) than to peak A_1 (33–46 °C; see Figure 6, trace d); and (2) both this temperature range of heat inactivation and peak A_2 change upon oxidation of cytochrome

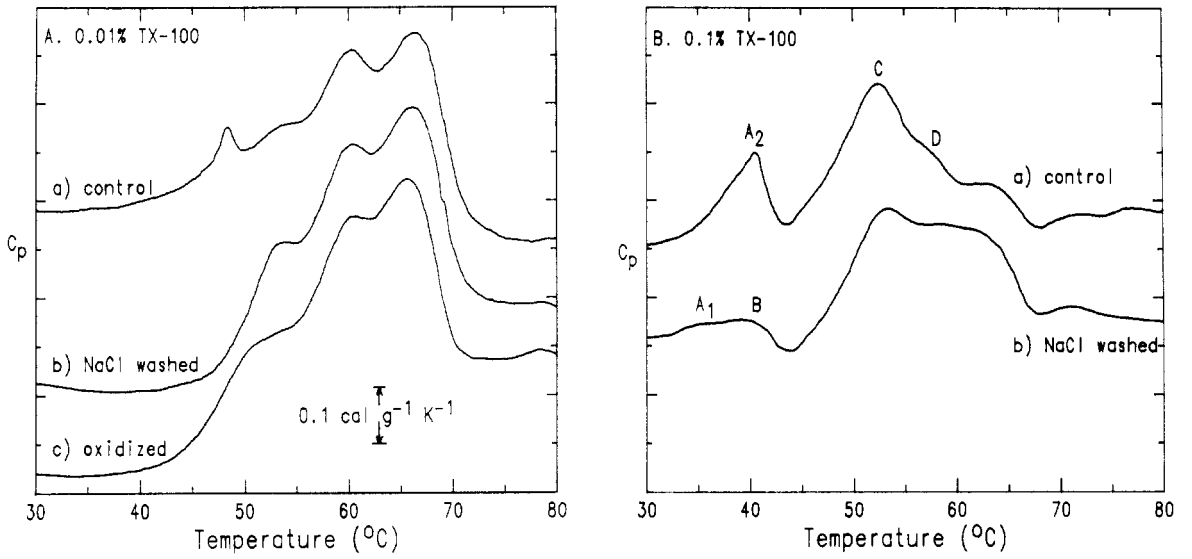

FIGURE 9: Effect of the removal of the 17- and 23-kDa polypeptides by 2 M NaCl washing on the DSC behavior. (A) PS II preparation 3 in pH 6 buffer plus 0.01% TX-100: (a) control; (b) 2 M NaCl treated; (c) 1 mM ferricyanide treated; 1.4–1.6 mg of Chl/mL. (B) PS II preparation 3 in pH 6 buffer plus 0.1% TX-100: (a) control and (b) NaCl treated; both 1.6 mg of Chl/mL.

b_{559} (see Figures 6 and 8), but there is no apparent change in peak A_1 (Figure 6). We conclude that peak A_2 corresponds to the functional denaturation of the OEC.

In order to use peak A_2 as a probe of the OEC, we have investigated the effects on the DSC trace of various treatments which perturb the OEC and have found several which perturb peak A_2. This peak is sensitive to the oxidation state of cytochrome b_{559}. Figure 6 shows the reversible removal of peak A_2, with no significant changes in the other resolved peaks, upon oxidation of cytochrome b_{559} with 1 mM ferricyanide and rereduction with 1 mM ascorbate. A heat inactivation experiment shows that activity is lost less sharply and at slightly lower temperature in PS II samples with cytochrome b_{559} oxidized than in control (cytochrome b_{559} reduced) samples (Figure 8). This broadened heat inactivation suggests that a parallel broadening of the very small A_2 peak may be the cause of its disappearance. Since the temperature range of heat inactivation of an oxidized sample (34–45 °C) is similar to that for peak A_1 (33–46 °C) and that of a reduced sample (38–46 °C) is similar to that for peak A_2 (40–45 °C), an alternate interpretation is that the denaturation of the OEC occurs during peak A_1 when cytochrome b_{559} is oxidized and during peak A_2 when it is reduced. However, it seems more plausible for the functional denaturation of the OEC to always occur during the same endothermic transition, A_2, which upon oxidation of cytochrome b_{559} becomes broadened and coincident with peak A_1.

Salt washing with 2 M NaCl, which is known to remove the 17- and 23-kDa polypeptides and decrease oxygen evolution activity to about 30% (Ghanotakis et al., 1984a), also removes peak A_2 (Figure 9A). However, this DSC effect is also related to the oxidation state of cytochrome b_{559}. The removal of these polypeptides has been shown to result in the conversion of high-potential cytochrome b_{559}, which is reduced under ambient redox conditions, to the low-potential forms (Larsson et al., 1984), which are oxidized under ambient redox conditions. Thus, peak A_2 disappears (it broadens, presumably) simply due to the oxidation of cytochrome b_{559}. Under these conditions (pH 6.0, 0.01% TX-100), peaks A_1 and A_2 are not resolved, so it is difficult to say whether one or both of these peaks are lost upon removal of the polypeptides. A similar experiment performed at 0.1% TX-100 (Figure 9B) shows that two broad peaks remain after the oxidation of cytochrome b_{559} by salt washing. This suggests that the large low-temperature peak is composed of three endothermic transitions, A_1, A_2, and B, and salt washing removes only one of them, the sharpest transition, A_2. The DSC effect of salt washing is equivalent to that of oxidation of cytochrome b_{559}, as shown in Figure 9A. Reconstitution of the 17- and 23-kDa polypeptides gives variable DSC traces: sometimes peak A_2 seems to return, but at lower temperatures (results not shown). This is consistent with the incomplete reconstitution of high-potential cytochrome b_{559} which accompanies rebinding of the 23-kDa polypeptide (Larsson et al., 1984). Addition of 5 mM $CaCl_2$, which reconstitutes about 80% activity in these salt-washed samples, does not affect the DSC trace. This is consistent with evidence that Ca^{2+} does not reconstitute the high-potential form of cytochrome b_{559} (Ghanotakis et al., 1986; Briantais et al., 1985).

Several other inhibitory treatments cause no DSC changes other than the loss of peak A_2 which accompanies oxidation of cytochrome b_{559}. Tris washing, which removes the 17-, 23-, and 33-kDa polypeptides and Mn and leaves no oxygen evolution activity (Kuwabara & Murata, 1983), gives a DSC trace identical with that produced by simply oxidizing cytochrome b_{559}. Since inhibition of the OEC may change only peak A_2, which seems to be too broad to observe when cytochrome b_{559} is oxidized, we have also investigated the DSC effects of inhibitory treatments which do not oxidize cytochrome b_{559}. Inhibition with 50 μM DCMU causes no significant changes in the DSC trace, perhaps because this treatment blocks electron transport on the electron acceptor side of PS II (Joliot & Kok, 1975) rather than altering the OEC and peak A_2. Ammonia is unique among the amines in that it inhibits oxygen evolution both by binding competitively with chloride (like the other amines) and by binding to another site, possibly the water binding site (Sandusky & Yocum, 1984; Beck et al., 1986). No significant changes occurred in the DSC trace upon addition of 100 mM NH_4Cl to samples in pH 7.5 buffer. The recent results of Nash et al. (1985), who showed that chloride depletion accelerates heat inactivation, suggest that this inhibitory treatment should alter peak A_2. Preliminary experiments indicate that chloride depletion causes significant changes in peak A_2, and further investigations of this effect are being pursued.

A comparison of the heat inactivation of the OEC with that

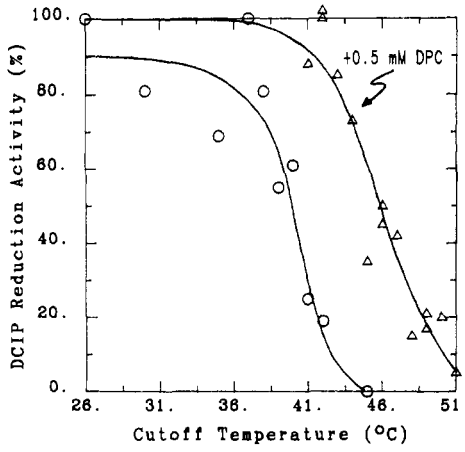

FIGURE 10: Heat inactivation of the photoreduction of DCIP: remaining activity (percent of control) vs. temperature at which the aliquot was withdrawn from the heating bath. Heat inactivation conducted at pH 7.5, 0.03% TX-100; activity assays in the absence (○) and presence (△) of the artificial electron donor DPC.

of the remainder of the electron-transport chain suggests that peak A_2 does not represent the denaturation of components critical to the entire chain. Figure 10 shows the results of a heat inactivation experiment where the samples were assayed for both types of activity by measuring the photoreduction of DCIP in the presence and in the absence of the artificial electron donor DPC. It is clear that under these conditions (pH 7.5, 0.03% TX-100) the OEC denatures at a lower temperature than the rest of the electron-transport chain, consistent with the results of Katoh and San Pietro (1967). As shown above for oxygen evolution activity, the loss of photoreduction of DCIP by water correlates with the DSC peak A_2 ($t_{1/2} \simeq$ 40 °C, t_m = 40.25 °C). Similarly, the loss of photoreduction of DCIP by DPC seems to correlate with the DSC peak B ($t_{1/2} \simeq$ 46 °C, $t_m \simeq$ 47.5 °C). This difference in the temperature of activity loss is quite small (1 °C) for samples at pH 6.0, 0.1% TX-100, consistent with the idea that the large low-temperature peak observed under these conditions is composed of the unresolved peaks A_1, A_2, and B. We have examined the correlation of peak B with heat inactivation of electron transport over a range of detergent concentrations (with experiments analogous to, but less extensive than, those done for peak A_2). When the results are plotted as in Figure 7 (not shown), a similar degree of correlation is observed. These results suggest that the denaturation of component(s) critical to electron transport occurs during peak B.

DISCUSSION

We have assigned parts of the DSC trace of photosystem II based on the effects of treatments and on correlations with heat inactivation. The enthalpy of denaturation for the entire complex, about 5–6 cal/g, is within the normal range observed for proteins (Privalov, 1979). The DSC trace is characterized by five major endothermic transitions, A_1, A_2, B, C, and D. None of the transitions were found to be reversible, also typical of many proteins. We suggest that peaks C and D are the denaturation profiles of the major component in these preparations, the LHCP. We assign peak A_2 to the functional denaturation of the OEC, that is, to the denaturation of at least some component(s) required for oxygen evolution activity. Peak B appears to represent the denaturation of components critical to the remainder of the electron-transport chain.

The DSC peaks C and D may provide insight into the various structural interactions mediated by the LHCP. Only one of the two peaks we have assigned to the LHCP, peak C, is affected by Mg. The other peak, D, appears to be highly sensitive to detergent, which causes it to broaden dramatically (see Figure 3). Perhaps this latter peak corresponds to the denaturation of an LHCP species which is not involved in the Mg-induced structural interactions but is instead involved in interactions which are quite easily disrupted by detergent. It would be quite interesting to examine the DSC curves of LHCP which have been isolated and reconstituted into liposomes. These membranes have been shown to be capable of cation-induced stacking (Mullet & Arntzen, 1980). This experiment could verify our assignment of the denaturation of the LHCP and investigate the function of the LHCP in mediating the interactions involved in the macroscopic structure of thylakoids.

We have focused our efforts on peak A_2 as a probe of the OEC. The heat inactivation experiments demonstrate that peak A_2 is the denaturation of protein(s) critical to oxygen evolution. This peak has two uniques features: its very small size and its extreme sharpness. Again assuming that the relative size of the DSC peak can be used as a rough indicator of the relative mass of the protein, this peak, with 2% of the total area, corresponds to the denaturation of approximately 20 kDa of protein. Since the high-potential to low-potential conversion of cytochrome b_{559} has been correlated with heat inactivation, and peak A_2 is sensitive to the state of cytochrome b_{559}, we suggest that this peak involves the denaturation of cytochrome b_{559}. The denaturation of two copies of cytochrome b_{559} per complex, each bound either by two copies of the 9-kDa polypeptide or by the 9- and the 4-kDa polypeptides, would correspond to 26–36 kDa of protein; this is compatible with our rough estimate of 20 kDa. The release of two Mn which seems to correlate with heat inactivation (Cramer et al., 1981; Nash et al., 1985) may actually be a part of the release of four Mn, occurring slightly after heat inactivation (and thus not during peak A_2), or may be part of the denaturation which is monitored by peak A_2.

The other unique feature of peak A_2, its sharpness, indicates that this is an extremely cooperative denaturation process. The parameter β, often interpreted to be the molecular weight of the cooperative unit (Sturtevant, 1974), is more than an order of magnitude higher than those of the other peaks (see Table I). Although a molecular weight of 3 million is clearly an overestimate of the size of the cooperative unit, it indicates that the denaturation of this component is unusually cooperative. Our heat inactivation results suggest that the disappearance of this peak upon oxidation of cytochrome b_{559} is due to broadening of the peak. Thus, this oxidation somehow disrupts the unusual cooperativity of the A_2 transition.

Before concluding that oxidation of cytochrome b_{559} drastically alters the denaturation of the OEC, it is important to consider whether some component other than cytochrome b_{559} is being affected by our treatments. A recent paper of Petroleas and Diner (1986) has shown that the electron acceptor side iron–quinone complex is oxidized by ferricyanide and rereduced by ascorbate. Although our similar redox treatment may also be affecting this complex, we argue that its redox changes are not responsible for the DSC changes in peak A_2 for the following reasons: (1) DCMU, which interacts with the electron acceptor side, does not change peak A_2; and (2) although there is evidence that salt washing alters the electron acceptor side (Wensink et al., 1984; Dekker et al., 1984), the results of de Paula et al. (1986) indicate that the iron has not been oxidized by this treatment, since a single light-induced charge separation (in the presence of DCMU) results in the g = 1.9 EPR signal associated with $Fe^{2+}Q_A^-$ at normal intensities. To the best of our knowledge, the only redox effect

of salt washing is the oxidation of cytochrome b_{559}, so that the common result of the two treatments which remove peak A_2 is the oxidation of cytochrome b_{559}.

All of the DSC effects of inhibitory treatments which we have discussed can be explained by a change in cytochrome b_{559}. Removal of the 17- and 23-kDa polypeptides causes no further changes in the DSC trace beyond that due to the oxidation of cytochrome b_{559}, suggesting that DSC is insensitive to changes in PS II due to the presence of these polypeptides. The same is true of the 33-kDa polypeptide and the Mn removed by Tris washing. Apparently, the denaturation of the extrinsic polypeptides is also not observed by DSC under our conditions. The presence of the inhibitors DCMU and NH_3 is also undetected by DSC. In all these cases, the absence of a component or the presence of an inhibitor may not cause a sufficiently large-scale change to be observed by DSC, or it may alter a peak which is masked by other transitions. Perhaps changes in cytochrome b_{559} are much more significant, in terms of macroscopic structure, than other changes caused by these treatments.

The chief evidence for the participation of cytochrome b_{559} in oxygen evolution is that many treatments which inactivate the OEC also convert cytochrome b_{559} from the native high-potential to the low-potential conformation. These treatments include addition of TX-100, heating, and aging (Cramer & Whitmarsh, 1977). Removal of the 17- and 23-kDa extrinsic polypeptides, which partially inactivates the OEC, results in a similar conversion (Larsson et al., 1984). It has been suggested that the binding of these polypeptides stabilizes the strained heme ligand conformation required to achieve the high potential (Babcock et al., 1985). Reconstitution of low-activity PS II preparations into liposomes has been found both to stimulate oxygen evolution and to increase the amount of high-potential cytochrome b_{559} (Butler & Matsuda, 1983). Additional evidence for the involvement of cytochrome b_{559} in oxygen evolution is that it is photooxidized at 77 K (Knaff & Arnon, 1969), suggesting that cytochrome b_{559} is in close proximity to the reaction center.

Despite these implications, there is no direct evidence for the participation of cytochrome b_{559} in oxygen evolution: no redox chemistry of cytochrome b_{559} has been observed to accompany oxygen evolution, and its potential (370 mV) is not consistent with a role in oxidizing water. There are several cases in which high oxygen evolution occurs in the apparent absence of high-potential cytochrome b_{559}. Trypsin treatment destroys high-potential cytochrome b_{559} well before destroying oxygen evolution activity. In greening leaves, the onset of PS II activity precedes the appearance of cytochrome b_{559} (Cramer & Whitmarsh, 1977). Another instance in which activity does not seem to require high-potential cytochrome b_{559} is that of salt-washed PS II samples, which are depleted of the 17- and 23-kDa polypeptides: 5 mM $CaCl_2$ reconstitutes 90% oxygen evolution activity but does not reconstitute high-potential cytochrome b_{559} (Ghanotakis et al., 1986; Briantais et al., 1985). This result has been used to argue against a role for cytochrome b_{559} in the OEC (Briantais et al., 1985).

Our DSC results suggest that the cooperativity of the A_2 transition is drastically altered by changes in the oxidation state of cytochrome b_{559}. Oxidation of cytochrome b_{559} somehow disrupts the intermolecular cooperativity of the denaturation of critical component(s) of the OEC, which suggests it plays a significant structural role in the oxygen-evolving complex of PS II.

ACKNOWLEDGMENTS

We thank J. F. Hershberger for his assistance with the digitization of the DSC data and W. F. Beck for his assistance with the software used to generate the figures.

Registry No. O_2, 7782-44-7; cytochrome b_{559}, 9044-61-5.

REFERENCES

Amesz, J. (1983) *Biochim. Biophys. Acta 726*, 1–12.

Armond, P. A., Björkman, O., & Staehelin, L. A. (1980) *Biochim. Biophys. Acta 601*, 433–442.

Babcock, G. T., Widger, W. R., Cramer, W. A., Oertling, W. A., & Metz, J. G. (1985) *Biochemistry 24*, 3638–3645.

Beck, W. F., de Paula, J. C., & Brudvig, G. W. (1985) *Biochemistry 24*, 3035–3043.

Beck, W. F., de Paula, J. C., & Brudvig, G. W. (1986) *J. Am. Chem. Soc. 108*, 4018–4022.

Berthold, D. A., Babcock, G. T., & Yocum, C. F. (1981) *FEBS Lett. 134*, 231–234.

Brandts, J. F., Erickson, L., Lysko, K., Schwartz, T. A., & Taverna, R. D. (1977) *Biochemistry 16*, 3450–3454.

Brandts, J. F., Taverna, R. D., Sadasivan, E., & Lysko, K. A. (1978) *Biochim. Biophys. Acta 512*, 566–578.

Briantais, J.-M., Vernotte, C., Miyao, M., Murata, N., & Picaud, M. (1985) *Biochim. Biophys. Acta 808*, 348–351.

Butler, W. L., & Matsuda, H. D. (1983) in *The Oxygen Evolving System of Photosynthesis* (Inoue, Y., et al., Eds.) p 113, Academic Press, Tokyo.

Chua, N.-H. (1980) *Methods Enzymol. 69*, 434–446.

Cramer, W. A., & Whitmarsh, J. (1977) *Annu. Rev. Plant Physiol. 28*, 133–172.

Cramer, W. A., Whitmarsh, J., & Low, P. S. (1981) *Biochemistry 20*, 157–162.

Critchley, C. (1985) *Biochim. Biophys. Acta 811*, 33–46.

Dekker, J. P., Ghanotakis, D. F., Plijter, J. J., Van Gorkom, H. J., & Babcock, G. T. (1984) *Biochim. Biophys. Acta 767*, 515–523.

de Paula, J. C., Innes, J. B., & Brudvig, G. W. (1985) *Biochemistry 24*, 8114–8120.

de Paula, J. C., Li. P. M., Miller, A.-F., Wu, B. W., & Brudvig, G. W. (1986) *Biochemistry* (in press).

Edge, V., Allewell, N. M., & Sturtevant, J. M. (1985) *Biochemistry 24*, 5899–5906.

Ghanotakis, D. F., Babcock, G. T., & Yocum, C. F. (1984a) *FEBS Lett. 167*, 127–130.

Ghanotakis, D. F., Topper, J. N., Babcock, G. T., & Yocum, C. F. (1984b) *FEBS Lett. 170*, 169–173.

Ghanotakis, D. F., Yocum, C. F., & Babcock, G. T. (1986) *Photosynth. Res. 9*, 125–134.

Gounaris, K., Brain, A. P. R., Quinn, P. J., & Williams, W. P. (1983) *FEBS Lett. 153*, 47–52.

Herrmann, R. G., Alt, J., Schiller, B., Widger, W. R., & Cramer, W. A. (1984) *FEBS Lett. 176*, 239–244.

Ikeuchi, M., Yuasa, M., & Inoue, Y. (1985) *FEBS Lett. 185*, 316–322.

Joliot, P., & Kok, B. (1975) in *Bioenergetics in Photosynthesis* (Govindjee, Ed.) p 387, Academic Press, New York.

Katoh, S., & San Pietro, A. (1967) *Arch. Biochem. Biophys. 122*, 144–152.

Knaff, D. B., & Arnon, D. I. (1969) *Proc. Natl. Acad. Sci. U.S.A. 63*, 956–962.

Kuwabara, T., & Murata, N. (1983) *Plant Cell Physiol. 24*, 741–747.

Lam, E., Baltimore, B., Ortiz, W., Chollar, S., Melis, A., & Malkin, R. (1983) *Biochim. Biophys. Acta 724*, 201–211.

Larsson, C., Jansson, C., Ljungberg, U., Åkerlund, H.-E., & Andersson, B. (1984) in *Advances in Photosynthesis Research I* (Sybesma, C., Ed.) p 363, Martinus Nijhoff/Dr. W. Junk Publishers, Dordrecht, The Netherlands.

Larsson, U. K., & Anderson, B. (1985) *Biochim. Biophys. Acta 809*, 396–402.
Ljungberg, U., Åkerlund, H.-E., & Andersson, B. (1984) *FEBS Lett. 175*, 255–258.
Lysko, K. A., Carlson, R., Taverna, R., Snow, J., & Brandts, J. F. (1981) *Biochemistry 20*, 5570–5576.
Manly, S. P., Matthews, K. S., & Sturtevant, J. M. (1985) *Biochemistry 24*, 3842–3846.
Melis, A., & Homann, P. H. (1978) *Arch. Biochem. Biophys. 190*, 523–530.
Miyao, M., & Murata, N. (1984) *FEBS Lett. 170*, 350–354.
Miyao, M., & Murata, N. (1985) *FEBS Lett. 180*, 303–308.
Mullet, J. E., & Arntzen, C. J. (1980) *Biochim. Biophys. Acta 589*, 100–117.
Nash, D., Miyao, M., & Murata, N. (1985) *Biochim. Biophys. Acta 807*, 127–133.
Petrouleas, V., & Diner, B. A. (1986) *Biochim. Biophys. Acta 849*, 264–275.
Privalov, P. L. (1979) *Adv. Protein Chem. 33*, 167–241.
Privalov, P. L. (1980) *Pure Appl. Chem. 52*, 479–497.
Sandusky, P. O., & Yocum, C. F. (1984) *Biochim. Biophys. Acta 766*, 603–611.
Sandusky, P. O., Selvius DeRoo, C. L., Hicks, D. B., Yocum, C. F., Ghanotakis, D. F., & Babcock, G. T. (1983) in *The Oxygen Evolving System of Photosynthesis* (Inoue, Y., et al., Eds.) p 189, Academic Press, Tokyo.
Satoh, K. (1983) in *The Oxygen Evolving System of Photosynthesis* (Inoue, Y., et al., Eds.) p 27, Academic Press, Tokyo.
Sturtevant, J. M. (1974) *Annu. Rev. Biophys. Bioeng. 3*, 35–51.
Sundby, C., & Andersson, B. (1985) *FEBS Lett. 191*, 24–28.
Tang, X.-S., & Satoh, K. (1985) *FEBS Lett. 179*, 60–64.
Wensink, J., Dekker, J. P., & Van Gorkom, H. J. (1984) *Biochim. Biophys. Acta 765*, 147–155.
Zuber, H. (1985) *Photochem. Photobiol. 42*, 821–844.

Location of the Sites of Reaction of *N*-Ethylmaleimide in Papain and Chymotryptic Fragments of the Gizzard Myosin Heavy Chain†

Narindar Nath,‡ Sumitra Nag, and John C. Seidel*

Department of Muscle Research, Boston Biomedical Research Institute, Boston, Massachusetts 02114, and Department of Neurology, Harvard Medical School, Boston, Massachusetts 02115

Received February 11, 1986; Revised Manuscript Received June 10, 1986

ABSTRACT: The thiol of the gizzard myosin heavy chain, which reacts most rapidly with *N*-ethylmaleimide (MalNEt), has been located in the subfragment 2 region of myosin rod by fragmentation of [^{14}C]-MalNEt-labeled myosin with papain and chymotrypsin. MalNEt reacts more slowly with thiols present in the 70- and 25-kilodalton (kDa) papain fragments of subfragment 1. The reaction of MalNEt with thiols present in these regions is increased on addition of ATP by factors of 2 and 10, respectively, when myosin is modified in 0.45 M NaCl where it is present in the extended, 6S conformation. The rate of increase of Mg^{2+}-activated adenosinetriphosphatase (ATPase) activity, which reflects the loss of ability of myosin to assume the folded, 10S conformation, and the rate of loss of K^+-EDTA-activated activity produced by MalNEt are both accelerated 5- to 10-fold on addition of ATP. The rates at which ATPase activities change agree closely to the reaction rates of MalNEt with the 25-kDa region of subfragment 1; therefore, the changes in these activities can be attributed to modification of a thiol of the 25-kDa segment. An increase in actin-activated ATPase activity produced by reaction of myosin with MalNEt in 0.45 M NaCl is accelerated by ATP by a factor of at least 4. Reaction with [^{14}C]MalNEt in the presence of MgATP and 0.2 M NaCl, where myosin is in the 10S form, inhibits the incorporation of radioactive MalNEt into the 25-kDa papain fragment of subfragment 1. It also prevents the increase in actin-activated ATPase activity and preserves the ability of myosin to assume the 10S form.

In reaching our present state of knowledge of the molecular basis of force generation, spectroscopic probes attached to the contractile proteins have played an important role, permitting investigation of structural changes and dynamic behavior of defined regions of these proteins (Morales et al., 1982; Gergely & Seidel, 1983). Cysteine residues, because of their chemical reactivity, have allowed attachment of probes at specific sites that can be defined in terms of their position in the amino acid sequence and eventually in the three-dimensional structure. The use of these sites has allowed estimates of intra- and intermolecular distances between sites on myosin and actin by spectroscopic (Burley et al., 1972; Marsh & Lowey, 1980; Takeshi et al., 1982) and chemical means (Reisler et al., 1974; Wells & Yount, 1979; Tao & Lamkin, 1981), leading to the proposal of a three-dimensional model of various reactive sites of the actin–S1 complex (Botts et al., 1984; dos Remedios & Cooke, 1984). The future usefulness of this approach will depend in part on the availability of additional sites for attachment of probes within the myosin and actin molecules.

Skeletal muscle myosin contains reactive thiols, SH-1 and SH-2 of the heavy chain (Kielley & Bradley, 1956), present in a 22-kDa tryptic peptide constituting the C-terminal region

†Supported by Grant HL-15391 from the National Institutes of Health and by a grant from the Muscular Dystrophy Association.
*Address correspondence to this author at Boston Biomedical Research Institute.
‡Present address: Department of Biochemistry, Punjab University, Chandigarh, India.

0006-2960/86/0425-6169$01.50/0